

## Original Research

# Transcriptional regulation of DLGAP5 by AR suppresses p53 signaling and inhibits CD8<sup>+</sup> T cell infiltration in triple-negative breast cancer

Qing Pan, Dachang Ma, Yi Xiao, Kun Ji, Jun Wu\*

Department of Galactophore, The First Hospital of Lanzhou University, Lanzhou 730000, PR China

## ARTICLE INFO

## Keywords:

TNBC  
AR  
DLGAP5  
p53 signaling pathway  
Tumor growth  
CD8<sup>+</sup> T cell infiltration

## ABSTRACT

Triple-negative breast cancer (TNBC) is a challenging subtype with unclear biological mechanisms. Recently, the transcription factor androgen receptor (AR) and its regulation of the DLGAP5 gene have gained attention in TNBC pathogenesis. In this study, we found a positive correlation between high AR expression and TNBC cell proliferation and growth. Furthermore, we confirmed DLGAP5 as a critical downstream regulator of AR with high expression in TNBC tissues. Knockdown of DLGAP5 significantly inhibited TNBC cell proliferation, migration, and invasion. AR was observed to directly bind to the DLGAP5 promoter, enhancing its transcriptional activity and suppressing the activation of the p53 signaling pathway. *In vivo* experiments further validated that downregulation of AR or DLGAP5 inhibited tumor growth and enhanced CD8<sup>+</sup> T cell infiltration. This study highlights the crucial roles of AR and DLGAP5 in TNBC growth and immune cell infiltration. Taken together, AR inhibits the p53 signaling pathway by promoting DLGAP5 expression, thereby impacting CD8<sup>+</sup> T cell infiltration in TNBC.

## Introduction

Triple-negative breast cancer (TNBC) is a particularly challenging subtype of breast cancer characterized by the absence of estrogen receptors (ERs), progesterone receptors (PRs), and human epidermal growth factor receptor-2 (HER-2) expression [1]. This aggressive form of breast cancer accounts for approximately 15–20 % of all breast cancer cases and is known for its heterogeneity, making it challenging to treat effectively [2,3]. Unfortunately, chemotherapy remains the primary treatment option for the majority of TNBC patients, despite its associated side effects and limited clinical success rates [4–7]. The overall survival rate at the five-year mark for TNBC patients stands at a discouraging 78.5 % [8]. Therefore, there is an urgent need to explore novel therapeutic targets to improve outcomes for TNBC patients.

Understanding the molecular mechanisms driving breast cancer progression is crucial for developing new therapeutic strategies [9]. One promising avenue of research in the context of TNBC is the androgen receptor (AR), a ligand-dependent transcription factor that plays a crucial role in regulating gene expression associated with breast cancer development [10–12]. Notably, positive AR expression has been detected in approximately 12–55 % of TNBC tumor samples, indicating its

potential significance in this subtype [13]. Recent studies have highlighted the pivotal role of AR and AR inhibitors in breast cancer [14]. While AR exhibits anti-tumor activity in ER-positive (ER+) breast cancer, its role in ER-negative (ER-) breast cancer, including TNBC, is more complex and may even stimulate tumor cell progression [14–16]. Consequently, AR is emerging as a novel molecular target for TNBC.

Emerging studies suggest that the transcription factor AR may play a significant role in TNBC by regulating various downstream genes [9,17]. The intriguing player in the TNBC landscape is DLGAP5, also known as hepatoma up-regulated protein (HURP). DLGAP5 functions as a signaling molecule with homology to the kinase domain of guanine nucleotide-binding protein-associated kinases, and it plays critical roles in various biological processes [18]. In multiple cancer types, including non-small cell lung cancer (NSCLC) and liver cancer, DLGAP5 has been linked to poor prognosis and is considered a diagnostic and prognostic biomarker [19,20]. Interestingly, research has shown that the inactivation of the DLGAP5 gene can inhibit the growth of breast cancer cells, potentially through effects on the cell cycle and mitochondrial autophagy [21]. Prior research has underscored the strong association of DLGAP5 with breast cancer development [22,23].

The protein p53 is another crucial player in cancer biology, capable

\* Corresponding author at: Department of Galactophore, The First Hospital of Lanzhou University, No.1 Donggang West Road, Lanzhou 730000, Gansu Province, China.

E-mail address: [ery\\_wujun@lzu.edu.cn](mailto:ery_wujun@lzu.edu.cn) (J. Wu).

<https://doi.org/10.1016/j.tranon.2024.102081>

Received 22 November 2023; Received in revised form 24 June 2024; Accepted 1 August 2024

Available online 24 August 2024

1936-5233/© 2024 The Authors. Published by Elsevier Inc. CC BY-NC license This is an open access article under the CC BY-NC license (<http://creativecommons.org/licenses/by-nc/4.0/>).

of regulating various biological processes in response to different cellular stress signals [24,25]. These stress signals can include oncogene activation, DNA damage, and replication stress [26]. Through post-translational modifications, p53 can activate specific cellular responses tailored to different stress types, thereby regulating the fate of cells [27]. Its impact on processes such as cell cycle arrest, DNA repair, apoptosis, invasion, and migration underscores its importance in cancer development [28]. Recent research has also highlighted p53's role in impeding tumor proliferation by controlling key enzymes in the glycolytic pathway, emphasizing its pivotal role in cancer development [29,30]. Of note, CD8<sup>+</sup> T cells have emerged as a significant factor in cancer prognosis, with a positive correlation observed in various tumor types [31]. Tumor neoantigens, which are tumor-specific antigens resulting from mutations in tumor cells, have garnered attention in cancer immunotherapy due to their strong immunogenicity and tumor-specific expression [32–34]. However, the interplay between AR, DLGAP5, the p53 signaling pathway, and immune cell infiltration, particularly CD8<sup>+</sup> T cells, remains poorly understood and warrants further investigation.

Our study aims to investigate the regulation of DLGAP5 expression by the transcription factor AR and its impact on the p53 signaling pathway and the infiltration of CD8<sup>+</sup> T cells in TNBC. Specifically, AR promoted the transcription of DLGAP5, which in turn downregulated the p53 signaling pathway, allowing for uncontrolled cell division and survival. Additionally, AR was observed to upregulate immunosuppressive factors such as IL-6 and IL-17, which affected the tumor immune microenvironment and further reduced CD8<sup>+</sup> T cell infiltration in TNBC. The molecular mechanisms of the AR/DLGAP5 axis in the immune regulation of TNBC were elucidated in this study to provide a theoretical basis for developing new therapeutic strategies against TNBC.

## Materials and methods

### Culture of cell lines

Human TNBC cell line MDA-MB-231 (HTB-26), mouse TNBC cell line 4T1 (CRL-2539), human normal breast epithelial cell line MCF-10A (CRL-10317), mouse breast epithelial cell line HC11 (CRL-3062), and human embryonic kidney cell line HEK293T (CRL-11268) were all procured from ATCC (USA). MDA-MB-231 cells were cultured in L15 medium (30–2008), 4T1 and HC11 cells in RPMI-1640 medium (30–2001), and HEK293T cells in DMEM medium (30–2002), all obtained from ATCC. The media were supplemented with 10 % FBS (10,099, Thermo Fisher, USA) and 1 % penicillin-streptomycin mix (P1400, Solarbio, China). MCF-10A cells were cultured in MEBM medium (CC-3150, Lonza, Switzerland) with the addition of 100 ng/mL cholera toxin (227,036, Merck, Germany). All cells were maintained in an incubator at 37°C with 5 % CO<sub>2</sub> and saturated humidity [35].

### Cell transfection

Lentiviral vectors pLKO were used to construct AR knockout (sh-AR) and DLGAP5 knockout (sh-DLGAP5) plasmids, with sequences provided in Table S1. During the preparation, 500 ng of target gene plasmid was mixed with 100  $\mu$ L of Opti-MEM, 50 ng of VSVG, 500 ng of pR8.74, and 3  $\mu$ L of transfection reagent polyethylenimine (HY-K2014, MedChemexpress, USA). The mixture was incubated for 15 min and then added to 12-well plates containing HEK293T cells at approximately 80 % confluence.

Three days post-transfection, the supernatant containing lentivirus was collected, filtered through a 0.45  $\mu$ m PES filter, and stored at –80 °C. Subsequently, MDA-MB-231 and 4T1 cells were seeded into 6-well plates. After 24 h, 50  $\mu$ L of virus solution (MOI=10, titer approximately 5  $\times$  10<sup>6</sup> TU/mL) and polybrene (1:1000) were added. After another day of infection, the medium was replaced with a fresh complete medium containing puromycin (HY-K1057, MedChemexpress, USA)

[20].

Overexpression vectors (oe-NC and oe-DLGAP5) were constructed using lentiviral vectors provided by Shanghai HanHeng Biotechnology. MDA-MB-231 and 4T1 cells, which were in good condition, highly viable, fully adherent, and 50 %–60 % confluent, were seeded into 6-well plates for lentiviral infection. After washing with PBS, the cells were incubated with serum-free L15 and 1640 medium containing polybrene (HY-112735, MedChemexpress, USA) diluted at 1:2000, with 1 mL of polybrene-containing medium added per well. Next, 15  $\mu$ L DLGAP5 overexpression lentivirus (oe-DLGAP5) or the corresponding volume of control lentivirus (oe-NC) were added according to the experimental groups. The plates were incubated for 6 h, after which 1 mL of L15 and 1640 medium containing 20 % serum was added per well. The medium was changed every 3 days, and the cells were cultured for 7 days [36].

### RT-qPCR

Total RNA was extracted from cells using Trizol reagent (15596018CN, Thermo Fisher, USA). The RT reactions were performed using HiScript® II RT SuperMix (R222-01, Vazyme Biotech Co., Ltd., Nanjing, China). The reaction mixtures were prepared using SYBR Green qPCR Mix (QPK-201, Toyobo, Shanghai, China), with  $\beta$ -actin serving as the internal control. The PCR program was designed as follows: initial denaturation at 98°C for 5 min, followed by 40 cycles of denaturation at 95°C for 10 s, annealing at 60°C for 30 s, and extension at 72°C for 20 s. A final hold was set at 12°C, followed by melting curve analysis. The relative mRNA expression levels were calculated using the 2<sup>– $\Delta\Delta$ CT</sup> method [37,38], and all experiments were repeated three times. Primer sequences are provided in Table S2.

### Western blot analysis

Total protein from cells or tissues was extracted using a total protein extraction kit (E-BC-E002, Elabscience Biotechnology Co., Ltd., Wuhan, China) and quantified using a BCA protein assay kit (P0012S, Beyotime Biotechnology, Shanghai, China). Protein sample were separated by denaturing SDS-PAGE (P0012A, Beyotime Biotechnology, Shanghai, China) and transferred onto methanol-activated PVDF membranes (LC2002, Thermo Fisher, USA). The membranes were then blocked with TBS containing 5 % non-fat milk and 1 % Tween-20. Primary antibodies were incubated overnight at 4°C (antibody details in Table S3). Following three washes with TBST (10 min each), the membranes were incubated with horseradish peroxidase-conjugated secondary antibodies at room temperature for 1 h, followed by three washes with PBST (10 min each). Bands were detected using enhanced chemiluminescence (ECL) reagent (P010, Beijing Applygen Technologies Co., Ltd., Beijing, China). Each sample was analyzed in triplicate [39].

### Chromatin immunoprecipitation (ChIP) assay

A ChIP assay was conducted using a ChIP kit (17–295, Millipore, USA) to investigate the enrichment of AR in the promoter region of the DLGAP5 gene. MDA-MB-231 and 4T1 cells were used, and when they reached 70–80 % confluency, they were fixed with 1 % formaldehyde at room temperature for 10 min to crosslink DNA and proteins. The cells were then sonicated to shear the chromatin into appropriate fragment sizes, with 10-second sonication pulses followed by 10-second intervals, repeated 15 times. The sonicated samples were centrifuged at 10,000 g at 4°C, and the supernatant was collected and divided into three tubes. These were incubated overnight at 4°C with positive control RNA polymerase II antibodies, negative control normal mouse IgG, and specific antibodies for the target protein (details in Table S4). Endogenous DNA-protein complexes were precipitated using Protein Agarose/Sepharose beads, briefly centrifuged, and the supernatant was discarded. Non-specific complexes were washed away, and crosslinks were reversed

by overnight incubation at 65°C. DNA fragments were purified using phenol/chloroform extraction. The enrichment of DLGAP5 sequences during immunoprecipitation was analyzed by real-time quantitative PCR (human: forward: 5'-CAATCGCAAGCCTGGTTGAG-3', reverse: 5'-CGCTGATTGGAGGGGCTTTA-3'; mouse: forward: 5'-ACACCTGTGATGACTCCCT-3', reverse: 5'-AGCTGTGCTGACCATGTGTT-3') [40].

#### Dual-Luciferase reporter assay

The potential binding sites of AR on DLGAP5 were predicted using the JASPAR database (<https://jaspar.genereg.net/>). The wild-type (WT, 5'-AGGGACAGAGACCTT-3' (human); 5'-GGGGACATGATCATCT-3' (mouse)) or mutant (Mut, 5'-GCCCTGTATCTGGAT-3' (human); 5'-CCCCTGTACTAGTAGGA-3' (mouse)) sequences of the DLGAP5 gene 3' untranslated region (3'UTR) were cloned into the pmirGLO luciferase reporter plasmid. The wild-type or mutant luciferase reporter plasmids were co-transfected with overexpression AR (sh-AR) or negative control (oe-NC) using Lipofectamine™ 3000 (L3000001, Invitrogen, USA). All plasmids were purchased from Guangzhou RiboBio Co., Ltd. Forty-eight hours post-transfection, the activities of firefly and Renilla luciferases were measured using the Dual-Luciferase Reporter Assay Kit (E1940, Promega, Beijing, China) and the relative luciferase activity was calculated [41].

#### CCK-8 assay

Cell viability was measured using the CCK-8 assay kit (C0038, Shanghai Biyuntian Biotechnology Co., Ltd., Shanghai, China). After 48 h of transfection, the cells were digested, and MDA-MB-231 and 4T1 cells were resuspended in L15 and MEM media, respectively. Subsequently, the cells were seeded at a density of  $3 \times 10^3$  cells per well in a 96-well plate. Cell viability was assessed by measuring the absorbance values at 24, 48, and 72 h after seeding. 10  $\mu$ L of CCK-8 solution was added to each well of a 96-well plate and incubated at 37°C for 2 h. The absorbance at 450 nm was measured using a microplate reader (A51119500C, ThermoFisher, USA) [42].

#### Flow cytometric apoptosis analysis

Transfected cells were collected by trypsinization, washed with cold PBS, and fixed with 70 % cold ethanol on ice for 30 min. For apoptosis analysis, the fixed cells were stained using the Annexin V-FITC/PI apoptosis detection kit (CA1020, Solarbio, Beijing, China) according to the manufacturer's instructions. Flow cytometry was performed using a FACS Calibur flow cytometer (342,973, BD, USA). The data were analyzed using Flow Jo™ v.10.8 software, with late apoptotic cells in the upper right quadrant and early apoptotic cells in the lower right quadrant [43].

#### Cell migration assay

MDA-MB-231 and 4T1 cells were counted to  $2.0 \times 10^5$  after digestion. Forty-eight hours post-transfection, when cells reached nearly 100 % confluency, a scratch was made using a 200  $\mu$ L pipette tip on the monolayer. Images were captured using an inverted microscope. The medium was replaced with a low-serum medium, and cells were incubated for another 24 h before capturing the images again [44].

#### Cell invasion assay

MDA-MB-231 and 4T1 cells were digested and centrifuged, with the supernatant discarded. Cells were resuspended in L15 and MEM media, respectively, followed by another round of centrifugation and washing. Matrigel (356,234, Corning, USA) was prepared at a 9:1 ratio of serum-free medium to Matrigel. Before the assay, 40  $\mu$ L of Matrigel was applied to the upper chamber of a Transwell insert. A total of  $1 \times 10^5$  cells in 200

$\mu$ L were seeded into the upper chamber, while 500  $\mu$ L of medium containing 10 % fetal bovine serum was added to the lower chamber. Cells were incubated at 37°C for 24 h. Non-invading cells were removed from the upper chamber, and the remaining cells were fixed with 70 % ethanol and stained with 0.5 % crystal violet for 10 min. Six random fields were selected to observe cell migration [45].

#### Single gene extraction for TNBC using the TCGA database

Data relevant to the TCGA-BRCA dataset were downloaded from The Cancer Genome Atlas (TCGA) database (<https://portal.gdc.cancer.gov/>). This dataset includes RNA sequencing data from 113 normal breast tissue samples and 1118 breast cancer tissue samples, along with clinical information from 1097 patients. Clinical information on ER, PR, and HER2 was extracted from TCGA XML files. Among the 1097 clinical cases, 220 cases were identified as ER- and PR-. After excluding 10 cases that were HER2 FISH-, the remaining cases were filtered based on the following criteria: (1) HER2 FISH status was negative, and HER2 IHC status was negative, equivocal, indeterminate, or unknown; or (2) HER2 IHC status was negative, HER2 FISH status was not positive, and HER2 IHC levels were 0, 1+, or unknown. From the filtered cases, only TCGA-AR-AOU1 lacked relevant RNA-seq gene expression data, resulting in the final retention of transcriptome data from 158 TNBC cases [46].

#### Construction of co-expression immune modules using WGCNA

The immune co-expression network was constructed using the "WGCNA" R package, following a workflow that includes gene co-expression network construction, module identification, module relationship analysis, and identification of highly correlated genes. The soft thresholding parameter was set to  $\beta = 9$ , and the scale-free  $R^2$  was set to 0.90. Key modules with the highest gene variability were selected, and the genes within these modules were used for subsequent analyses [47–49].

#### Immune infiltration analysis

Immune infiltration analysis was performed on the TCGA data using the immune infiltration scoring tool available on the Sangerbox website, employing the "CIBERSORT" algorithm. "CIBERSORT" is a deconvolution algorithm that uses gene expression data to describe the cell composition of complex tissues, allowing for the calculation of the relative proportions of infiltrating immune cells in patient tissues. Samples with a  $P$ -value < 0.05 were considered more reliable for analysis. The R package "Vioplot" was used to visualize the proportion of infiltrating immune cells in samples, comparing the immune cell content between high and low DLGAP5 expression groups [50].

#### High-Throughput transcriptome sequencing, data quality control, and differential gene analysis

Three MDA-MB-231 cell samples with sh-NC (knockdown control) and three samples with sh-AR (knockdown AR) were prepared. Total RNA was extracted from each sample using Trizol reagent (Thermo Fisher, USA, Cat# 16096020). RNA concentration, purity, and integrity were measured using a Qubit® 2.0 fluorometer with the Qubit® RNA Assay Kit (Thermo Fisher, USA, Cat# HKR2106-01), a NanoDrop spectrophotometer, and the RNA Nano 6000 Assay Kit for the Bioanalyzer 2100 system (Agilent, USA, Cat# 5067-1511).

For RNA sample preparation, 3  $\mu$ g of total RNA from each sample was used as input material. cDNA libraries were generated using the NEB-Next® Ultra™ RNA Library Prep Kit for Illumina® (NEB, Beijing, China, Cat# E7435L) following the manufacturer's recommendations. Library quality was assessed using the Agilent Bioanalyzer 2100 system. Indexed samples were clustered using the TruSeq PE Cluster Kit v3-cBot-HS (Illumina, USA, Cat# PE-401-3001) on a cBot cluster generation

system. Sequencing was performed on the Illumina HiSeq 550 platform to obtain 125 bp/150 bp paired-end reads [51,52].

Quality control of the raw sequencing data was conducted using FastQC software v0.11.8. Preprocessing of raw data was done with Cutadapt software v1.18 to remove Illumina sequencing adapters and poly(A) tails. Reads with over 5% N content were filtered out using Perl scripts. Reads with more than 70 % base quality above 20 were retained using the FASTX Toolkit v0.0.13. Paired-end reads were repaired using BMAP software. Filtered high-quality reads were then aligned to the human reference genome using hisat2 software v0.7.12.

Differentially expressed genes (DEGs) between sh-NC and sh-AR samples were identified using the "Limma" package in R, with thresholds set at  $|\log_{2}FC| > 1$  and  $P$ -value  $< 0.05$ . Heatmaps of DEG expression were generated using the "heatmap" package in R, and volcano plots were created using the "ggplot2" package. GO and KEGG enrichment analyses were performed using the "clusterProfiler" package in R [53, 54].

#### Establishment of mouse 4T1 xenograft model

A total of 48 female BALB/c mice, aged 4–6 weeks, were purchased from Beijing Vital River Laboratory Animal Technology Co., Ltd. (Beijing, China). The mice were housed in an SPF-grade animal laboratory with humidity maintained at 60 % to 65 % and temperature at 22°C to 25°C. After one week of acclimation, the experiment commenced following a health assessment of the mice. All experiments involving mice were approved by the Animal Ethics Committee of the First Hospital of Lanzhou University.

The 4T1 cells ( $1 \times 10^6$ ) were subcutaneously injected into the fourth mammary fat pad of the BALB/c mice. The experiment was divided into two parts. In the first part, the effect of DLGAP5 knockdown on immune infiltration was evaluated with the following groups: (1) sh-NC group (injected with 4T1 cells transduced with sh-NC lentivirus) and (2) sh-DLGAP5 group (injected with 4T1 cells transduced with sh-DLGAP5 lentivirus).

The second part investigated the impact of AR/DLGAP5 on immune infiltration, with the following groups: (1) sh-NC + oe-NC group (injected with 4T1 cells transduced with sh-NC + oe-NC lentivirus), (2) sh-AR + oe-NC group (injected with 4T1 cells transduced with sh-AR + oe-NC lentivirus), and (3) sh-AR + oe-DLGAP5 group (injected with 4T1 cells transduced with sh-AR and oe-DLGAP5 lentivirus). After euthanasia, the size and weight of the tumors were measured, and tumor volume was calculated using the formula  $(L \times W^2)/2$  (L: length; W: width) [55].

#### Immunohistochemical detection

Paraffin-embedded tissue sections were subjected to deparaffinization, rehydration, and antigen retrieval. Sections were incubated with 3 % hydrogen peroxide at room temperature, followed by overnight incubation at 4°C with DLGAP5 antibody (1:200, Wuhan Abebio Science Co., Ltd., Hubei, China) in a humidified chamber. The next day, sections were incubated with goat anti-rabbit IgG (1:500, Bioss, Beijing, China). After PBS washes, sections were treated with horseradish peroxidase-labeled reagent (Abcam, Cat# ab6721, UK). DAB was used for color development, followed by hematoxylin counterstaining, phenolization, dehydration, clearing, and mounting. Observations and photographs were taken using a light microscope [42].

#### Flow cytometry analysis of Treg cells and CD8<sup>+</sup> T cells in mouse tumor tissue

The proportion of Treg cells and the levels of CD8<sup>+</sup> T cells in mouse tumor tissue were analyzed using flow cytometry. Tumor tissues were excised from mice and minced using surgical scissors. The minced tissues were then homogenized on ice and filtered through a 70 µm Falcon

cell strainer. The collected cell suspension was treated with red blood cell lysis buffer to stop the reaction, followed by centrifugation to remove the supernatant. This process was repeated twice. The cell suspension was resuspended in PBS buffer and passed through a 40 µm Falcon cell strainer to remove cell clumps. The filtered cell suspension was then adjusted to a concentration of  $5 \times 10^9$  to  $1 \times 10^{10}$  cells/L and transferred to appropriate flow cytometry tubes.

To identify Treg cells, the following antibodies from Biolegend (USA) were used: Percp-labeled anti-mouse CD4 (0.25 µg, Cat# 100432), PE-labeled anti-mouse CD3 (0.25 µg, Cat# 100206), FITC-labeled anti-mouse CD8 (0.25 µg, Cat# 140403), PE-labeled anti-mouse CD25 (0.25 µg, Cat# 113704), and Alexa Fluor 488-labeled anti-mouse Foxp3 (0.25 µg, Cat# 126406). Corresponding isotype control antibodies (0.25 µg each, Cat# 400630, 400508, 4006250) were added to the control tubes.

The proportion of Treg cells in tumor tissue was determined using a flow cytometer. Fresh tumor tissues from each mouse were ground and digested at 4°C. Flow cytometry was used to measure the levels of CD4<sup>+</sup> T cells, CD8<sup>+</sup> T cells, and their secretion of IFN-γ in tumor tissues from each group of mice. The antibodies used included CD4 (Cat# ab207755) and CD8 (Cat# ab217344) from Abcam (UK), and the IFN-γ antibody (Cat# 12-7311-82) from eBioscience (USA) [56].

#### ELISA

Serum samples (20 µL each) were collected from each mouse. The levels of IL-6 and IL-17 in the serum were measured using ELISA kits according to the manufacturer's instructions (IL-6: E-EL-M2453c, IL-17: E-EL-M0047c, Elabscience Biotechnology Co., Ltd., Hubei, China) [57].

#### Statistical analysis

Data analysis and graph generation were performed using GraphPad Prism 8.0.2 software. All experiments were independently repeated three times. Quantitative data that followed a normal distribution were presented as mean ± standard deviation. A  $t$ -test was used for comparisons between two groups, while one-way analysis of variance (ANOVA) was employed for comparisons among multiple groups. A  $P$ -value  $< 0.05$  was considered statistically significant.

#### Results

##### AR Inhibition Suppresses Proliferation, Migration, and Invasion while Promoting Apoptosis in TNBC Cells

To investigate the regulatory mechanism of AR in TNBC, we conducted initial examinations of AR expression levels in human normal breast cells (MCF-10A), human TNBC cells (MDA-MB-231), mouse normal breast cells (HC11), and mouse TNBC cells (4T1) utilizing Western blot and RT-qPCR. The results showed that the AR was highly expressed in TNBC cells, as depicted in Fig. 1A-B and Figure S1A-B. To explore the impact of AR on breast cancer, we performed knockdown experiments to suppress the AR expression and analyzed AR levels in MDA-MB-231 and 4T1 cells. The results from Western blot and RT-qPCR (Fig. 1C-D; Figure S1C-D) demonstrated that sh-AR effectively suppressed the expression of the AR gene in both cell types, indicating the successful induction of low target gene expression through lentiviral transfection.

The results from the CCK-8 experiments and flow cytometry revealed that knockdown of AR substantially reduced the proliferation capabilities of MDA-MB-231 and 4T1 cells while increasing cell apoptosis (Fig. 1E-F; Figure S1E-F). The migration and invasion assay results indicated that knocking down AR decreased migratory and invasive potential of MDA-MB-231 and 4T1 cells compared to the control group (Fig. 1G-H; Figure S1G-H).

In conclusion, the inhibition of AR could suppress the proliferation, migration, and invasion abilities of TNBC cells while simultaneously promoting cell apoptosis.

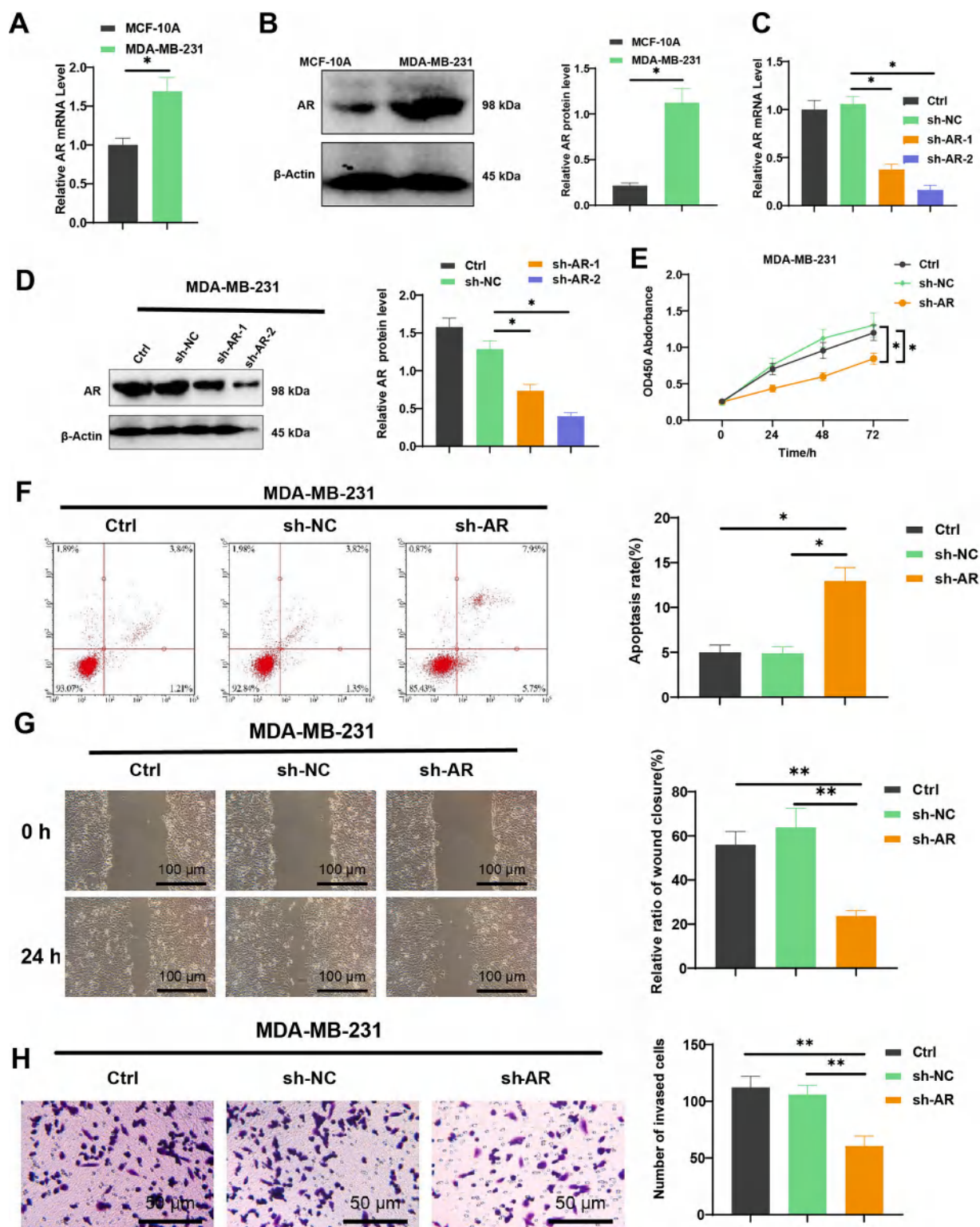


**Fig. 1.** Effects of AR knockdown on TNBC cells. *Note:* (A) Protein expression levels of AR in MCF-10A and MDA-MB-231 cells were detected using Western blot. (B) mRNA expression levels of AR in MCF-10A and MDA-MB-231 cells were detected using RT-qPCR. (C) Changes in AR mRNA expression in MDA-MB-231 cells after AR knockdown were detected using RT-qPCR. (D) Changes in AR protein expression in MDA-MB-231 cells after AR knockdown were detected using Western blot. (E) Changes in the proliferation capacity of MDA-MB-231 cells after AR knockdown were detected using CCK-8 assay. (F) Changes in the apoptosis of MDA-MB-231 cells after AR knockdown were detected using flow cytometry. (G) Changes in the migration ability of MDA-MB-231 cells after AR knockdown were tested using scratch assay. (H) Changes in the invasion ability of MDA-MB-231 cells after AR knockdown were tested using Transwell assay. \*  $p < 0.05$ ; all cell experiments were repeated 3 times.

### DLGAP5 Identified as a Potential Downstream Regulatory Gene of AR in TNBC

To further investigate the underlying mechanisms of AR in TNBC (TNBC), we conducted transcriptomic sequencing and differential analysis on sh-NC and sh-AR transfected MDA-MB-231 cells. One hundred thirty-three DEGs, consisting of 88 upregulated and 45 downregulated genes, were identified (Figure S2A). The significance level was set at  $|\log_{2}FC| > 1$  and  $p < 0.05$ . The KEGG analysis revealed that these genes are enriched in pathways such as p53 signaling, cell adhesion molecules (CAMs), and the cell cycle (Fig. 2A).

Moreover, we conducted a differential expression analysis using the TCGA database. 159 TNBC samples were selected and compared to normal control samples with a log fold change greater than 2 and a  $p$ -value lower than 0.05. This analysis identified 2151 DEGs, comprising 1441 upregulated genes and 710 downregulated genes (Figure S2B).

Subsequently, we performed co-expression analysis using WGCNA on these genes and employed  $r^2=0.9$  and  $\beta=9$  as the thresholds for module identification. The corresponding results are displayed in Figure S2C. Following hierarchical clustering analysis, we identified 9 co-expression gene modules (Fig. 2B). The blue, yellow, and turquoise modules exhibited high gene significance scores (Fig. 2C). The genes in the blue module were positively correlated with TNBC, whereas those in the yellow module were negatively correlated with TNBC (Fig. 2D). Furthermore, the blue module's module membership was positively correlated with gene significance, whereas no correlation is observed in the yellow module (Fig. 2E). Henceforth, we chose 479 genes from the blue module for further analysis.

We conducted a differential analysis using the GSE58135 dataset obtained from the GEO database. The dataset consisted of 21 cases of adjacent cancer tissue and 42 cases of TNBC tissue, with second-generation sequencing data available ( $|\log_{2}FC| > 2$ ,  $p < 0.05$ ). From this analysis, we identified a total of 2137 DEGs. The results indicated 690 upregulated genes and 1447 downregulated genes regarding expression (Figure S2D). We identified seven intersecting genes, namely CDK1, CHEK1, DLGAP5, PLK1, GTSE1, CCNB1, and CDKN2A, through the intersection of the blue module genes derived from TCGA-TNBC data, DEGs from GSE58135 chips, and DEGs obtained from sequencing MDA-MB-231 cells after AR knockdown (Fig. 2F; Figure S2E). Of these genes, DLGAP5 is the gene that shows the most downregulation in MDA-MB-231 cells, which interferes with AR (Fig. 2G).

Furthermore, our analysis of TCGA-TNBC samples indicates an upregulation of the target gene DLGAP5 in TNBC breast cancer tissue compared to normal control tissue. Furthermore, by utilizing TCGA data from the Ualcan database, we observed a notably higher expression of DLGAP5 in TNBC when compared to normal control tissues (Fig. 2H-I). Furthermore, based on the KM-plot N data analysis, high expression of DLGAP5 was linked to reduced overall survival (OS) and recurrence-free survival (RFS) in breast cancer, with HR (95 % CI) values of 2.13 (1.9–2.39) and 2.25 (1.74–2.92) respectively. This association was observed in Fig. 2J.

Hence, we hypothesized that DLGAP5 might potentially function as a downstream regulatory gene of AR, influencing the development of TNBC. Furthermore, AR might impact the p53 signaling pathway.

### DLGAP5 Knockdown Impedes TNBC Cell Proliferation, Migration, and Invasion while Enhancing Apoptosis

To further investigate the role of DLGAP5 in TNBC, we performed experiments to generate cell lines with DLGAP5 knockdown. Firstly, the knockdown efficiency of DLGAP5 was validated. The results from RT-qPCR and Western blot analysis (Fig. 3A-B; Figure S3A-B) demonstrated that both sh-DLGAP5-1 and sh-DLGAP5-2 effectively reduced the mRNA and protein expression levels of the DLGAP5 gene, confirming the successful establishment of a DLGAP5 knockdown cell line.

The CCK-8 experimental results (Fig. 3C; Figure S3C) demonstrated a decrease in the proliferation ability of 4T1 and MDA-MB-231 cells after transfection with sh-DLGAP5. Moreover, the inhibitory effect was more pronounced with sh-DLGAP5-2, leading to the selection of cells

transfected with sh-DLGAP5-2 for subsequent experiments. Flow cytometry analysis showed that the depletion of DLGAP5 led to enhanced apoptosis in 4T1 and MDA-MB-231 cells (Fig. 3D; Figure S3D). The results of the invasion and migration experiments revealed a decrease in the migration and invasion of MDA-MB-231 and 4T1 cells following the downregulation of DLGAP5, as compared to the sh-NC group (Fig. 3E-F; Figure S3E-F).

The findings above suggest that the downregulation of DLGAP5 could impede the proliferation, migration, and invasion of TNBC cells while promoting apoptosis.

### Suppression of DLGAP5 Modulates Tumor Microenvironment and Promotes CD8<sup>+</sup> T Cell Infiltration in TNBC

The analysis of the tumor microenvironment and immune infiltration using TCGA data and the CIBERSORT algorithm revealed a negative correlation between high DLGAP5 expression and the content of CD8<sup>+</sup> T cells ( $p < 0.01$ ), as depicted in Fig. 4A. Further construction of 4T1 tumor model for transplantation validation. Initially, the impact of DLGAP5 knockdown through lentiviral transduction was assessed using immunohistochemistry (Fig. 4B). The results demonstrated a decrease in DLGAP5 expression level in the sh-DLGAP5 group instead of the sh-NC group, indicating the successful depletion of DLGAP5 in the 4T1 tumor model. Compared to the sh-NC group, the tumor size decreased in the sh-DLGAP5 group, suggesting that the downregulation of DLGAP5 could inhibit TNBC tumor growth (Fig. 4C).

Treg cells represent a specific subset of T cells that exert profound immunosuppressive effects [58]. This study revealed the involvement of DLGAP5 in the immune response by assessing Treg cells' enrichment level. Compared to the sh-NC group, the sh-DLGAP5 group exhibited a reduction in the level of Treg cells within the tumor tissue. This difference was statistically significant, suggesting that the suppression of DLGAP5 expression could enhance the immunosuppressive effect (Fig. 4D). CD8<sup>+</sup> T cells and CD4<sup>+</sup> T cells are effector cells that play a role in the anti-tumor response within the tumor microenvironment. The sh-DLGAP5 group exhibited a substantial increase in CD8<sup>+</sup> T/CD4<sup>+</sup> T cells, compared to the sh-NC group, as demonstrated by Fig. 4E.

IFN- $\gamma$  is a pro-inflammatory cytokine released by CD4<sup>+</sup> T cells, CD8<sup>+</sup> T cells, or natural killer cells. It is crucial in mediating cellular immune responses and exhibits diverse effects, including immunoregulatory, anti-tumor, and antiviral activities [59]. There were no differences in the levels of IFN- $\gamma$  among the groups, as observed in CD4<sup>+</sup> T cells (Fig. 4F). Moreover, the levels of IFN- $\gamma$  in CD8<sup>+</sup> T cells from the sh-DLGAP5 group exhibited an increase compared to the control group, as depicted in Fig. 4G.

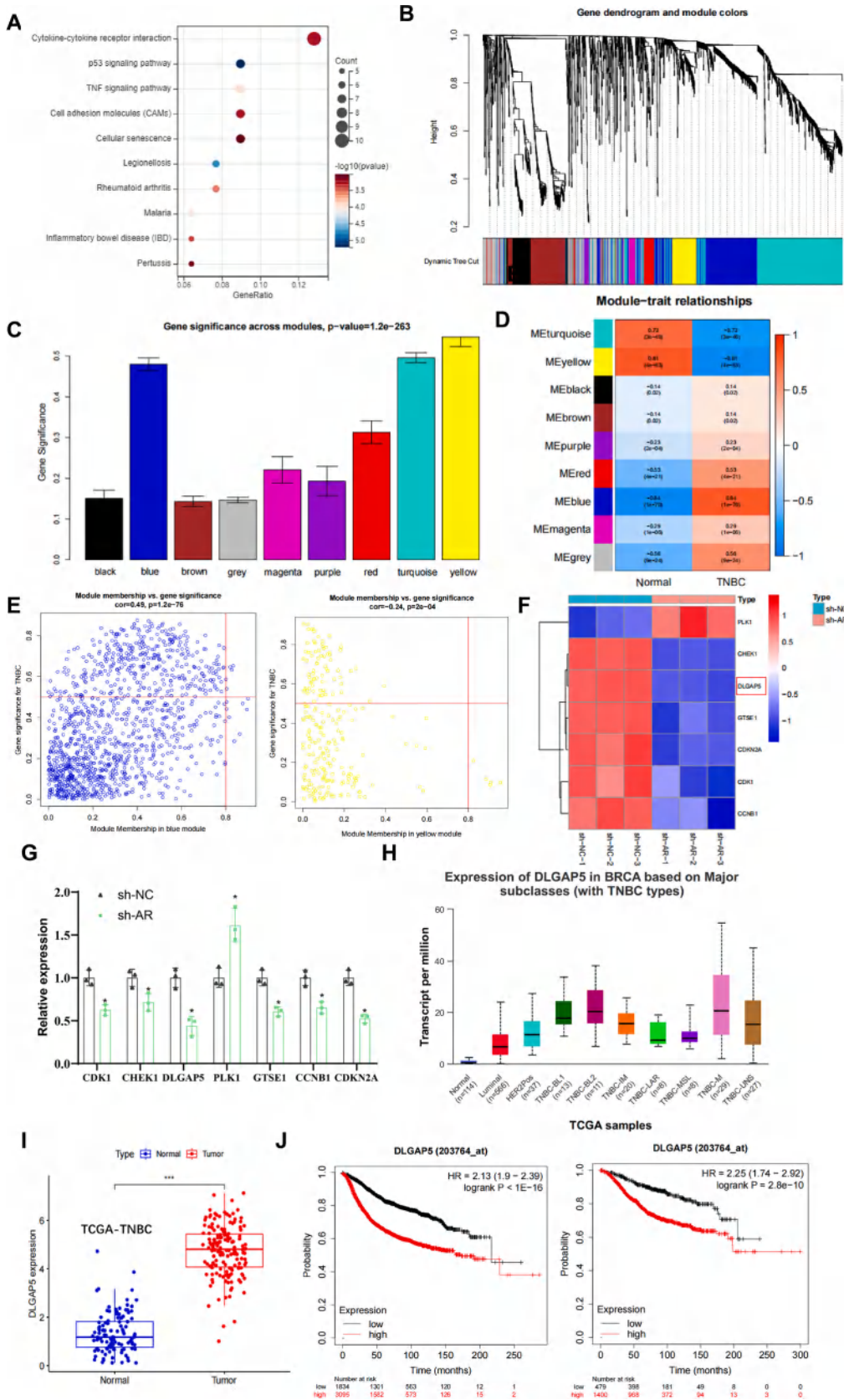
IL-6 and IL-17 play crucial roles in tumor immune evasion, closely associated with the incidence and progression of diverse malignancies, impeding the body's anti-tumor responses [60,61]. Compared to the sh-NC group, the serum levels of IL-6 and IL-17 in the sh-DLGAP5 group decreased significantly (Fig. 4H). This result suggested that the downregulation of DLGAP5 decreased the levels of IL-6 and IL-17, thereby enhancing immune function.

In conclusion, the suppression of DLGAP5 potentially enhanced the tumor microenvironment and promoted the infiltration of CD8<sup>+</sup> T cells into tumor tissues.

### AR Directly Targets and Enhances DLGAP5 Expression, Modulating the p53 Pathway in TNBC Cells

Further analysis was conducted to illuminate the regulatory mechanism of AR on DLGAP5. We searched the NCBI database for the corresponding sequence to identify the binding sites within the DLGAP5 promoter region. Subsequently, we utilized the JASPAR database to predict the binding sites in both human and mouse DLGAP5 promoter regions (Fig. 5A-B). Relevant primers were designed based on these sequences. The chromatin immunoprecipitation (ChIP) analysis revealed the enrichment of AR binding in the DLGAP5 promoter region (Fig. 5C; Figure S4A).

To validate if AR directly targets the DLGAP5 promoter, we generated a luciferase promoter vector for DLGAP5 and co-transfected it with



(caption on next page)

**Fig. 2.** Investigation of the regulatory mechanism of AR in TNBC based on transcriptome sequencing. *Note:* (A) Evaluation of DEGs involved in KEGG pathways in MDA-MB-231 cells through knockdown with sh-NC or sh-AR in transcriptome sequencing. (B) WGCNA co-expression analysis of DEGs in 159 TNBC samples and 113 normal control samples selected from the TCGA database, resulting in a cluster dendrogram and a trait heatmap, with each leaf in the cluster dendrogram corresponding to a different gene module. (C) Assessment of gene importance scores in the modules of the dataset. (D) Presentation of the correlation heatmap between modules in the dataset and TNBC, with each cell containing the corresponding correlation and *P*-value. (E) Analysis of the correlation between the blue and yellow modules and gene importance. (F) Heatmap showing differential expression of 7 overlapping genes in transcriptome sequencing of MDA-MB-231 cells after knockdown with sh-NC or sh-AR. (G) Presentation of the differential expression of 7 overlapping genes in transcriptome sequencing of MDA-MB-231 cells after knockdown with sh-NC or sh-AR. (H) Presentation of the expression of DLGAP5 in different subtypes in the Ualcan database. (I) Presentation of the expression of DLGAP5 in the Normal group ( $n = 113$ ) and Tumor group ( $n = 158$ ) in the TCGA database. (J) Research on breast cancer prognosis about DLGAP5 expression through KM-plotter online data analysis (left for RFS, right for OS). \*  $p < 0.05$ , \*\*  $p < 0.001$ .

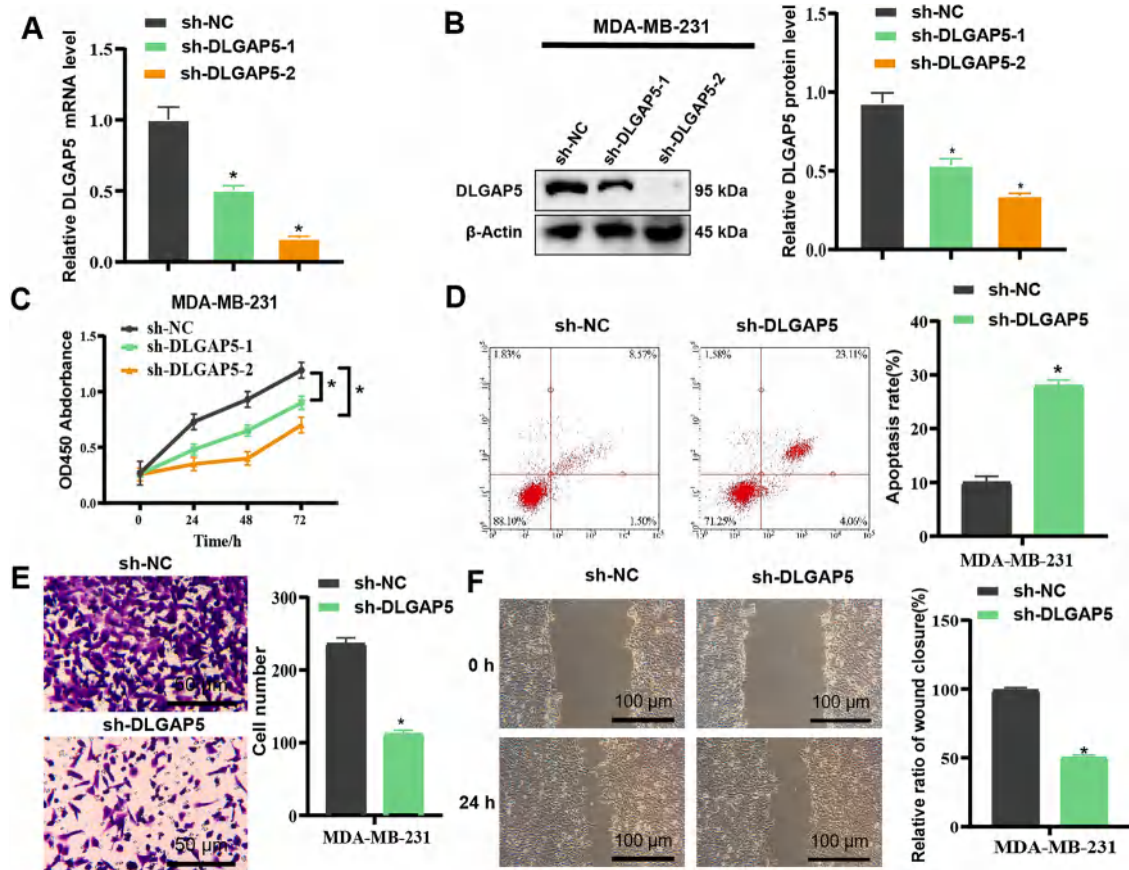


**Fig. 3.** Effects of DLGAP5 knockdown on MDA-MB-231 cells. *Note:* (A) Changes in DLGAP5 mRNA expression in MDA-MB-231 cells after transfection with sh-DLGAP5 were detected using RT-qPCR. (B) Changes in DLGAP5 protein expression in MDA-MB-231 cells after DLGAP5 knockdown were detected using Western blot. (C) Changes in the proliferation capacity of MDA-MB-231 cells after transfection with sh-DLGAP5 were detected using CCK-8 assay. (D) Changes in the apoptosis of MDA-MB-231 cells after DLGAP5 knockdown were detected using flow cytometry. (E) Changes in the invasion ability of MDA-MB-231 cells after DLGAP5 knockdown were tested using Transwell assay. (F) Changes in the migration ability of MDA-MB-231 cells after DLGAP5 knockdown were tested using scratch assay. \*  $p < 0.05$ ; all cell experiments were repeated 3 times.

an AR knockdown vector into TNBC cells. The analysis of luciferase activity indicated that the downregulation of AR increased the promoter activity of DLGAP5 in TNBC cells (Fig. 5D; Figure S4B). The findings demonstrate that the AR can enhance the expression of DLGAP5 in TNBC cells. p-p53 represents the active state of p53, and an elevated p-p53/p53 ratio signifies p53 activation. Western blot analysis (Fig. 5E) revealed that the downregulation of DLGAP5 in MDA-MB-231 and 4T1 cells markedly upregulated p21 expression and the p-p53/p53 ratio, suggesting that DLGAP5 knockdown could activate the p53 pathway in TNBC cells, potentially inhibiting the malignant phenotype of TNBC. After validation of the knockdown of AR and the overexpression of DLGAP5, the levels of p53 pathway-related proteins were measured (Fig. 5F; Figure S4C-D). The results indicated that the knockdown of AR increased the values of p21 and p-p53/p53, whereas the overexpression of DLGAP5 reversed this effect. These findings suggested a synergistic

regulatory effect of AR and DLGAP5 on p53. The AR activated the p53 pathway by inhibiting the expression of DLGAP5.

#### *In vivo validation of the AR/DLGAP5/p53 axis modulating TNBC tumor growth in mouse xenograft model*

We investigated the *in vivo* role of the AR/DLGAP5/p53 axis in the TNBC mouse xenograft model. The results demonstrated that the suppression of AR reduced tumor growth compared to the sh-NC+oe-NC group. However, this trend was reversed by the overexpression of DLGAP5 (Fig. 6A-C).

Furthermore, we quantified the mRNA and protein expression levels of various factors in tumor tissues of tumor-bearing mice *in vivo* using RT-qPCR and Western blot analysis. The results demonstrated that in the sh-AR+oe-NC group, there was a downregulation in both the mRNA and

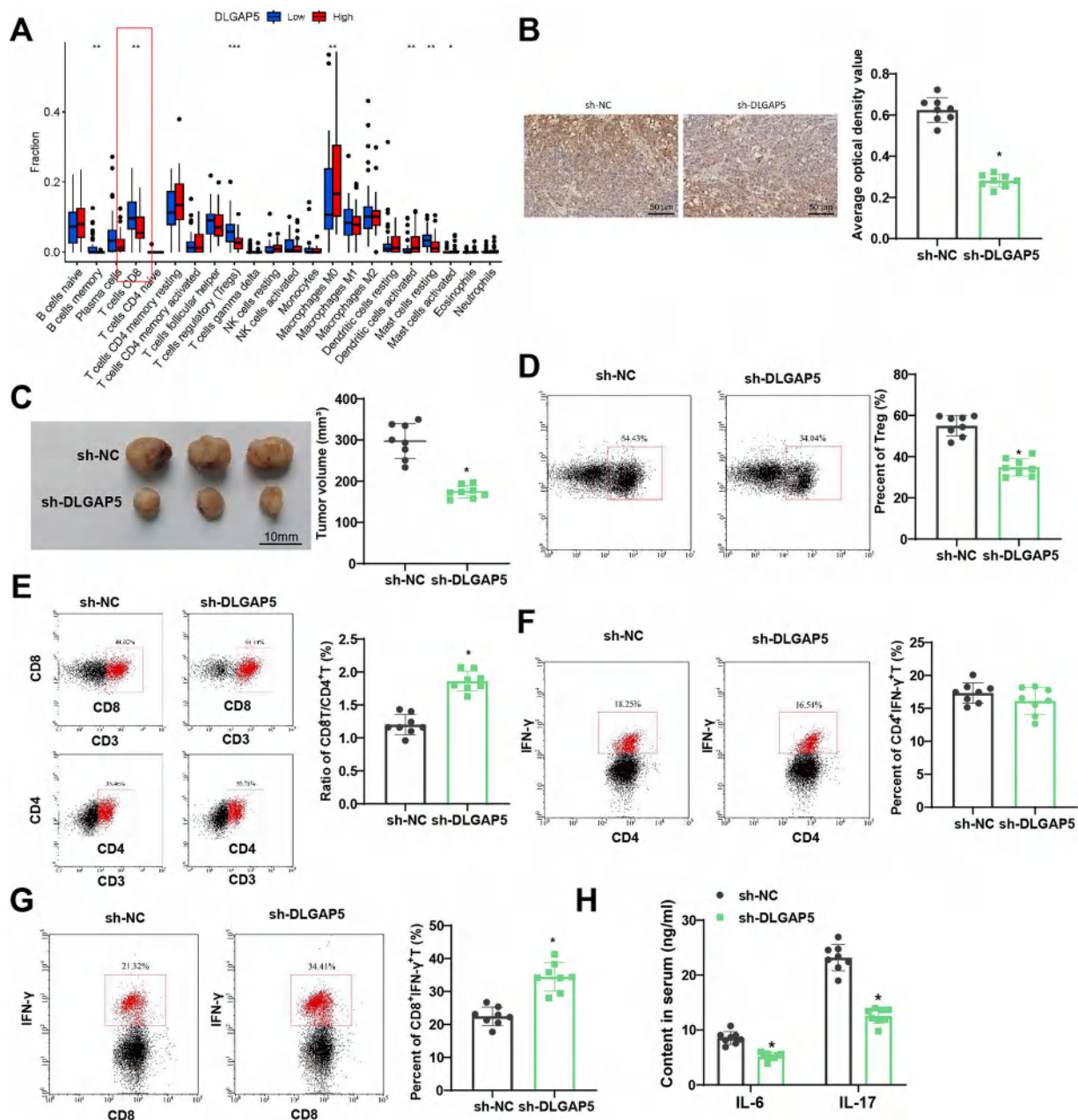


**Fig. 4.** Effects of DLGAP5 knockdown on immune regulation in tumor-bearing mice. *Note:* (A) Analysis of immune cell infiltration in TCGA-TNBC data when analyzing the high and low expression of DLGAP5 based on the median of DLGAP5 gene expression. (B) Expression of DLGAP5 in tumor tissues of different groups of mice was detected using immunohistochemistry. (C) Illustration of tumor size and tumor volume in different groups of mice. (D) Levels of Treg cells in transplant tumor tissues of different groups of mice were detected using flow cytometry. (E) Expression of CD4<sup>+</sup> T and CD8<sup>+</sup> T cells in tumor tissues of different groups of mice was detected using flow cytometry. (F) Levels of IFN- $\gamma$  in CD4<sup>+</sup> T cells of different groups of mice were detected using flow cytometry. (G) Levels of IFN- $\gamma$  in CD8<sup>+</sup> T cells of different groups of mice were detected using flow cytometry. (H) Levels of IL-6 and IL-17 in the serum of different groups of mice were detected using an ELISA kit. \*  $p < 0.05$ , \*\*  $p < 0.01$ , all cell experiments were repeated 3 times, and animal experiments had 8 mice in each group.

protein expression of AR and a downregulation in the mRNA and protein stability of DLGAP5. However, following the overexpression of DLGAP5, the expression level of DLGAP5 was increased, exhibiting no difference compared to the Model group (Fig. 6D-E). The results suggested that the expression of DLGAP5 was downregulated in tumor-bearing mice with AR knockdown.

Simultaneously, we assessed the expression levels of proteins related to p53 in tumor tissues. The results demonstrated that AR depletion enhanced the expression of the p21 protein, thereby increasing the p-p53/p53 ratio (Fig. 6F). Following the overexpression of DLGAP5, this trend was reversed, providing further evidence that AR activates the p53 signaling pathway by regulating DLGAP5, thereby exerting an anti-

tumor effect.

**AR Suppression Modulates DLGAP5 Expression and Enhances Immune Response in TNBC Tumor-Bearing Mice**

To investigate the impact of AR on immune infiltration through the regulation of DLGAP5, a total of three groups were formed in 4T1 tumor-bearing mice: (1) sh-NC+oe-NC group, (2) sh-AR+oe-NC group, and (3) sh-AR+oe-DLGAP5 group. Flow cytometry analysis detected that sh-AR inhibited the expression of Treg cells compared to the oe-NC group, as shown in Fig. 7A. Additionally, it led to an increase in the ratio of CD8<sup>+</sup>T/CD4<sup>+</sup>T. In contrast, the expression of DLGAP5 exhibits an opposite trend (Fig. 7B). No differences were observed in the levels of IFN- $\gamma$  in CD4<sup>+</sup> T cells among the different groups (Fig. 7C).

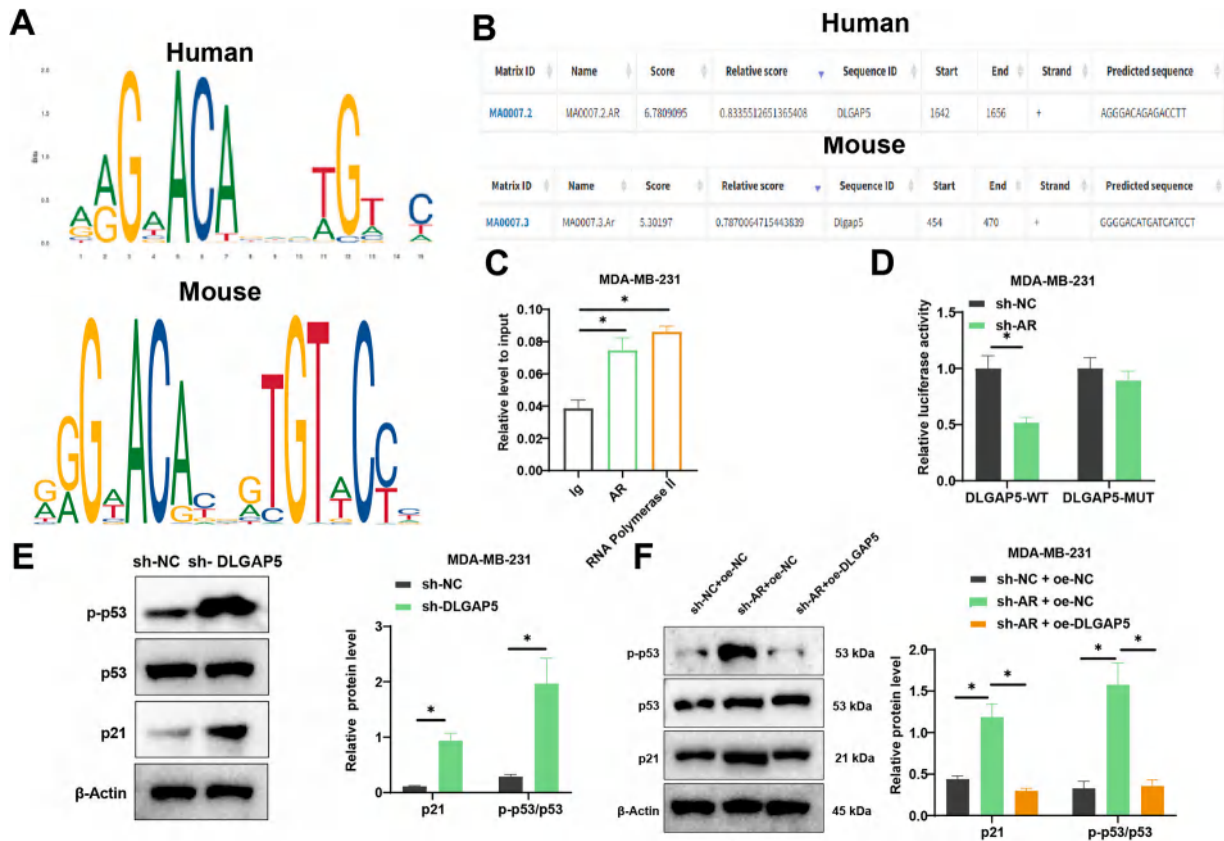


**Fig. 5.** Activation of the p53 signaling pathway by the transcriptional regulation of DLGAP5 by AR. *Note:* (A) Schematic illustration of AR binding sites. (B) AR binding sites in the promoter region of AR and DLGAP5. (C) CHIP assay analyzes the binding of the DLGAP5 promoter region to AR in MDA-MB-231 and 4T1 cells. (D) Comparison of relative luciferase activity of different groups in MDA-MB-231 and 4T1 cells using a dual-luciferase reporter assay. (E) Changes in the expression of p-p53, p53, and p21 proteins in MDA-MB-231 cells after transfection with sh-DLGAP5 were detected using Western blot. (F) Changes in the expression of p-p53, p53, and p21 proteins in MDA-MB-231 cells after transfection with sh-AR and oe-DLGAP5 were detected using Western blot. \*  $p < 0.05$ , \*\*  $p < 0.01$ , all cell experiments were repeated 3 times.

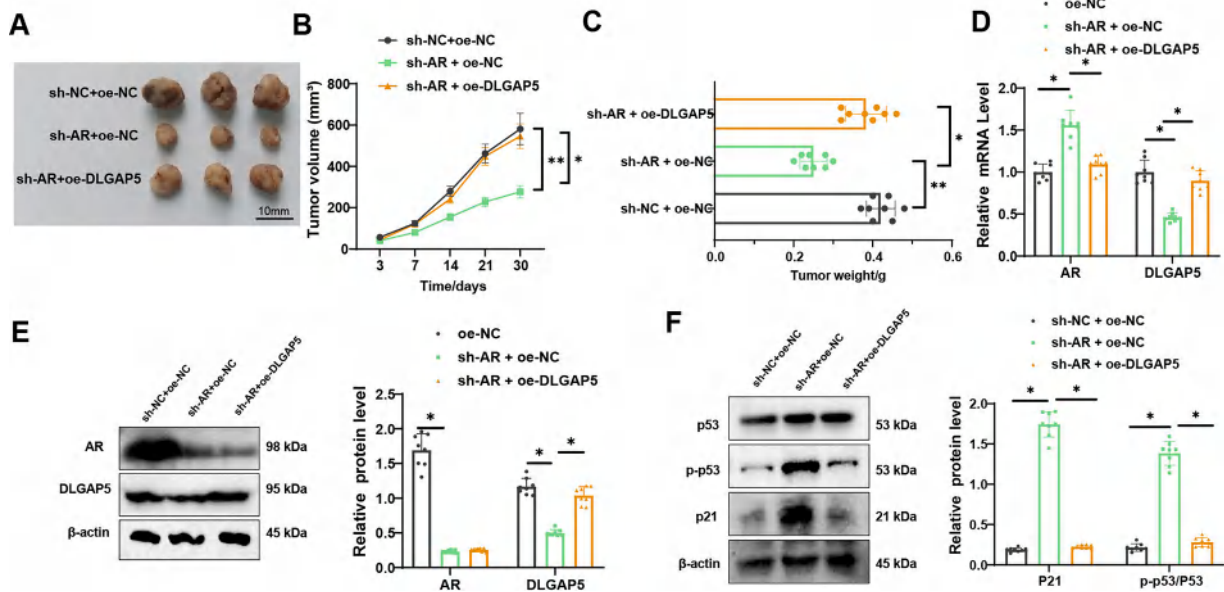


**Fig. 6.** Effects of AR knockdown or DLGAP5 overexpression on tumor growth in tumor-bearing mice. *Note:* (A) Effects of AR knockdown and DLGAP5 overexpression on tumor volume in tumor-bearing mice. (B) Changes in tumor growth in different groups of tumor-bearing mice. (C) Changes in tumor weight in different groups of tumor-bearing mice. (D) mRNA expression levels of AR and DLGAP5 in tumor tissues of tumor-bearing mice were detected using RT-qPCR. (E) Protein expression levels of AR and DLGAP5 in tumor tissues of tumor-bearing mice were detected using Western blot. (F) Protein expression levels of p-p53, p53, and p21 in tumor tissues of tumor-bearing mice were detected using Western blot. \*  $p < 0.05$ , \*\*  $p < 0.01$ , there were 8 mice in each group.

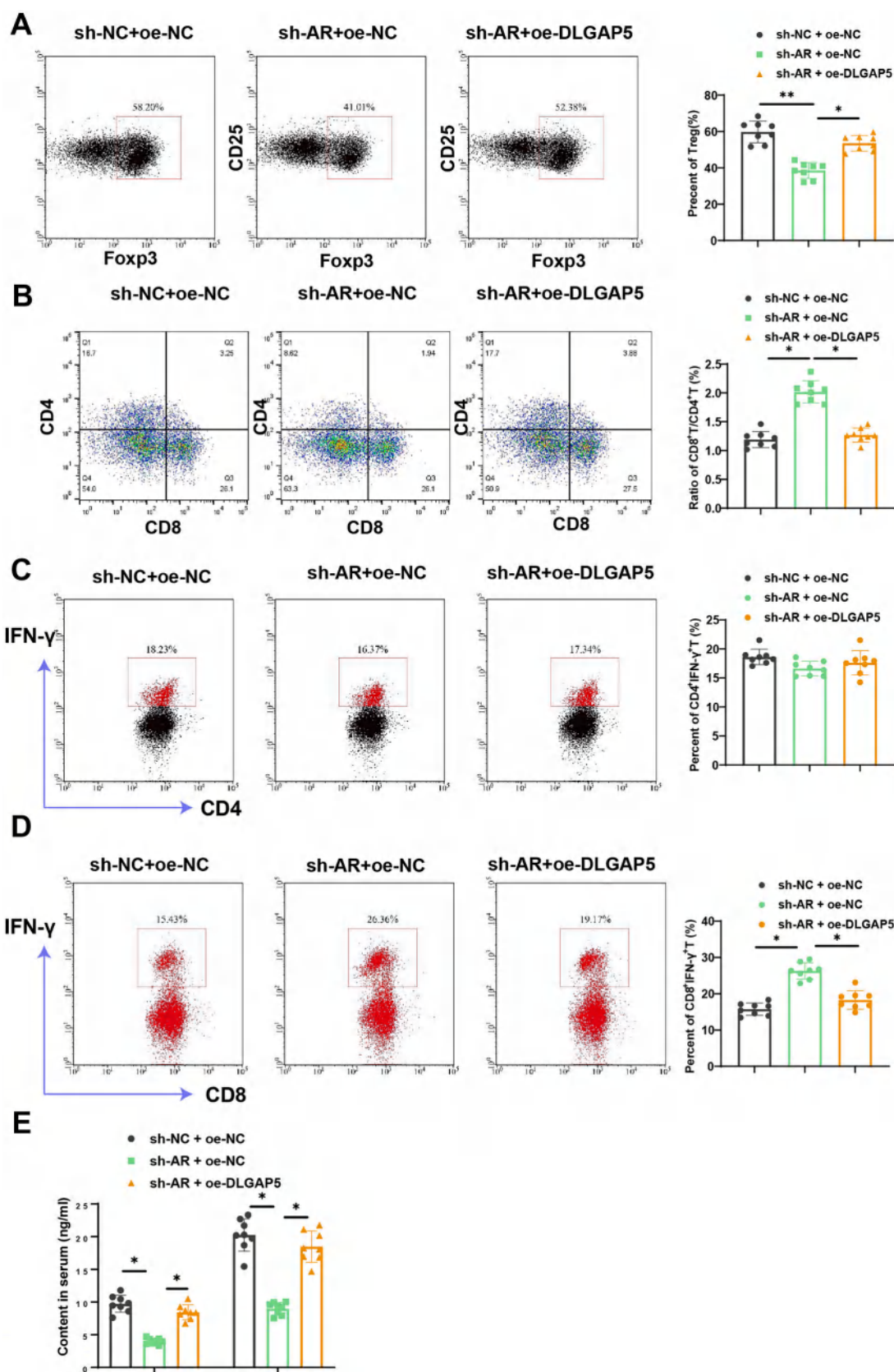


**Fig. 7.** AR-mediated DLGAP5 increases CD8<sup>+</sup> T cell immune infiltration in tumor tissue. *Note:* (A) Flow cytometry was used to measure the level of Treg cells in tumor tissue of each group of mice; (B) Flow cytometry was used to measure the change in the ratio of CD8<sup>+</sup> T cells to CD4<sup>+</sup> T cells in tumor-bearing mice of each group; (C) Flow cytometry was used to measure the level of IFN-γ secretion by CD4<sup>+</sup> T cells in tumor-bearing mice of each group; (D) Flow cytometry was used to measure the level of IFN-γ secretion by CD8<sup>+</sup> T cells in tumor-bearing mice of each group; (E) ELISA assay was used to measure the levels of IL-6 and IL-17 in the serum of each group of mice. \* *p* < 0.05, and \*\* *p* < 0.01; each group consisted of 8 mice.

In tumor tissue, the sh-AR group promotes the release of IFN- $\gamma$  in CD8<sup>+</sup> T cells compared to the oe-NC group, whereas overexpression of DLGAP5 leads to decreased levels of IFN- $\gamma$  (Fig. 7D). In the sh-AR group, the levels of IL-6 and IL-17 in the serum decreased, whereas they increased following the overexpression of DLGAP5 (Fig. 7E).

The results suggest that suppressing AR could regulate DLGAP5 and augment the immune response to tumors in TNBC mice.

## Discussion

TNBC is characterized by aggressive biological behavior, limited treatment options, and a poor prognosis [3,62]. The infiltration of immune cells, particularly CD8<sup>+</sup> T cells, is pivotal in tumor suppression in this specific type of cancer [63]. However, regulating the infiltration and activation of CD8<sup>+</sup> T cells remains critical for treating TNBC [64]. This study presents a novel mechanism by which the transcription factor AR regulates the expression of DLGAP5, influencing the p53 signaling pathway and thereby suppressing CD8<sup>+</sup> T cell infiltration.

The role of AR has been validated in numerous tumors in previous studies. However, its specific mechanism in TNBC remains unclear [65, 66]. Our findings indicate that AR directly modulates the expression of DLGAP5, subsequently impacting the p53 signaling pathway. This research contributes to a novel comprehension of the functional localization of AR in TNBC.

DLGAP5 is overexpressed in TNBC and a variety of other tumors [21]. This finding suggests it could be a prevalent oncogenic driver [67]. However, the mechanism by which DLGAP5 regulates tumor proliferation, migration, and invasion and its relationship with other signaling pathways, such as p53, remains unclear in previous studies [68]. Our experimental findings demonstrated a negative correlation between DLGAP5 and the p53 signaling pathway, suggesting that overexpression of DLGAP5 could result in the inactivation of the p53 signaling pathway, consequently facilitating tumor growth.

The p53 protein plays a fundamental role as a 'guardian of the genome' by ensuring genomic stability and preventing the formation of tumors [69]. Our experimental data demonstrates that DLGAP5 can suppress the activation of the p53 signaling pathway. It offers a fresh perspective to further investigate how different oncogenic genes regulate the p53 signaling pathway.

TNBC is more susceptible to immune cell infiltration than other breast cancer types [70]. Our research has established the mechanism by

which inhibiting the AR/DLGAP5 axis reduces CD8<sup>+</sup> T cell infiltration. Specifically, the downregulation of AR or DLGAP5 appears to enhance the tumor immune microenvironment, making it more conducive to immune cell infiltration. This modulation results in increased infiltration of CD8<sup>+</sup> T cells and the production of IFN- $\gamma$ , while reducing immunosuppressive cells such as Tregs and factors such as IL-6 and IL-17. These changes suggest that targeting AR or DLGAP5 can shift the balance towards a more immunogenic environment, enhancing immune surveillance and antitumor activity in TNBC. This mechanism underscores the potential therapeutic benefits of modulating the AR/DLGAP5 axis to improve immune infiltration and combat TNBC progression. Further research is needed to fully elucidate these pathways and their implications for treatment strategies.

Based on the results above, we could tentatively conclude that the transcription factor AR activates the expression of DLGAP5, leading to the suppression of the p53 signaling pathway activation, inhibition of CD8<sup>+</sup> T immune cell infiltration, and promotion of TNBC growth (Fig. 8). This study unveils the influence of the transcription factor AR on the expression of DLGAP5 and its impact on CD8<sup>+</sup> T cell infiltration, mediated by the p53 signaling pathway. It provides a novel theoretical foundation for understanding the molecular-level occurrence and development of TNBC. Elucidating this mechanism not only enhances our comprehension of the pathogenesis of breast cancer but also introduces novel targets for future therapeutic interventions.

TNBC presents a considerable challenge in terms of treatment. This study elucidated the roles of AR and DLGAP5 in the proliferation of TNBC cells, offering valuable guidance for targeted therapeutic approaches. There is optimism that developing novel drugs or treatments could enhance the therapeutic efficacy of TNBC. Furthermore, this study has revealed the significance of the AR/DLGAP5 axis in regulating the immune response to tumors. This study suggests that manipulating this axis could potentially impact the tumor immune microenvironment, presenting novel targets for immunotherapy in the future.

Although this study provides a new molecular theoretical basis for understanding the mechanisms of immune regulation in TNBC, some limitations remain. This study utilized only MDA-MB-231 and 4T1 cells for *in vitro* experiments, limiting the representation of the diversity within TNBC. Subsequent research should incorporate multiple cell lines specific to TNBC to validate the experimental findings. Moreover, this study primarily examined the regulation of DLGAP5 on CD8<sup>+</sup> T immune cells. Nonetheless, the immunoregulatory mechanisms of TNBC may

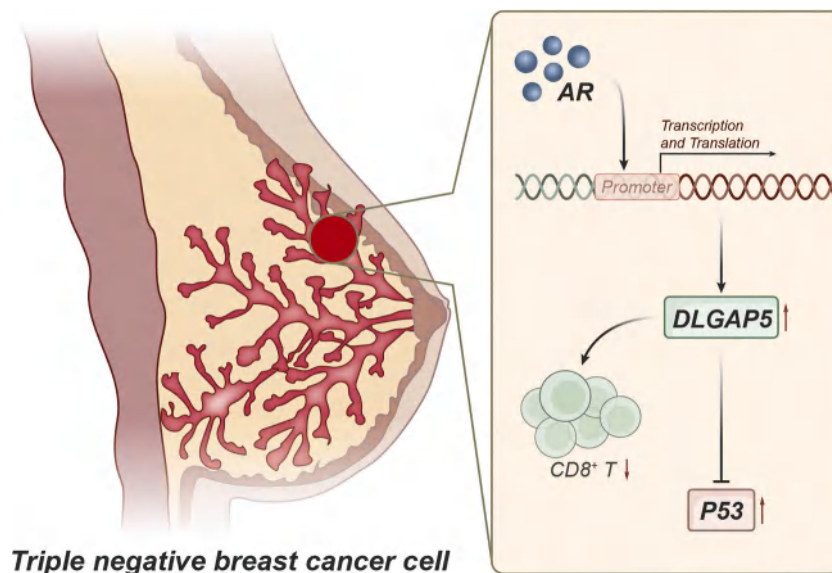


**Fig. 8.** Schematic representation of the potential molecular mechanisms. Transcription factor AR regulates the expression of DLGAP5 and represses the p53 signaling pathway, thereby modulating CD8<sup>+</sup> T cell infiltration and the tumor microenvironment in TNBC.

encompass additional signaling pathways and molecular mechanisms. Moreover, the presence of additional unknown mechanisms that may affect the AR/DLGP5/p53 signaling pathway requires further investigation. Simultaneously, future drug development focusing on this signaling axis may be crucial in offering more precise and effective treatment alternatives for patients with TNBC.

### Ethical statement

All experiments involving mice were approved by the Animal Ethics Committee of the First Hospital of Lanzhou University.

### CRedit authorship contribution statement

**Qing Pan:** Writing – original draft, Methodology, Data curation, Conceptualization. **Dachang Ma:** Validation, Software, Methodology. **Yi Xiao:** Visualization, Investigation, Data curation. **Kun Ji:** Writing – review & editing, Writing – original draft, Project administration, Funding acquisition. **Jun Wu:** Writing – review & editing, Writing – original draft, Project administration.

### Declaration of competing interest

The author declares no conflict of interest.

### Funding

This study was supported by Lanzhou Municipal Bureau of Science and Technology(2022-ZD-95) and Lanzhou University First Hospital Intramural Fund (ldyyyn2020-44).

### Acknowledgment

None.

### Supplementary materials

Supplementary material associated with this article can be found, in the online version, at [doi:10.1016/j.tranon.2024.102081](https://doi.org/10.1016/j.tranon.2024.102081).

### References

- [1] L. Yin, J.J. Duan, X.W. Bian, S.C. Yu, Triple-negative breast cancer molecular subtyping and treatment progress, *Breast Cancer Res.* 22 (1) (2020) 61, <https://doi.org/10.1186/s13058-020-01296-5>.
- [2] M.J. Armstrong, M.S. Okun, Diagnosis and treatment of parkinson disease: a review, *JAMA* 323 (6) (2020) 548–560, <https://doi.org/10.1001/jama.2019.22360>.
- [3] J.Y. So, J. Ohm, S. Lipkowitz, L. Yang, Triple negative breast cancer (TNBC): non-genetic tumor heterogeneity and immune microenvironment: emerging treatment options, *Pharmacol. Ther.* 237 (2022) 108253, <https://doi.org/10.1016/j.pharmthera.2022.108253>.
- [4] W.B. El Gazzar, K.A. Albakri, H. Hasan, A.M. Badr, A.A. Farag, O.M. Saleh, Poly (ADP-ribose) polymerase inhibitors in the treatment landscape of triple-negative breast cancer (TNBC), *J. Oncol. Pharm. Pract.* 29 (6) (2023) 1467–1479, <https://doi.org/10.1177/10781552231188903>.
- [5] D.D. Singh, D.K. Yadav, TNBC: potential targeting of multiple receptors for a therapeutic breakthrough, nanomedicine, and immunotherapy, *Biomedicines* 9 (8) (2021) 876, <https://doi.org/10.3390/biomedicines9080876>. Published 2021 Jul 23.
- [6] J. Jin, Z. Tao, J. Cao, T. Li, X. Hu, DNA damage response inhibitors: an avenue for TNBC treatment, *Biochim. Biophys. Acta Rev. Cancer* 1875 (2) (2021) 188521, <https://doi.org/10.1016/j.bbcan.2021.188521>.
- [7] Y. Li, H. Zhang, Y. Merkher, et al., Recent advances in therapeutic strategies for triple-negative breast cancer, *J. Hematol. Oncol.* 15 (1) (2022) 121, <https://doi.org/10.1186/s13045-022-01341-0>.
- [8] H. Wang, X. Rong, G. Zhao, et al., The microbial metabolite trimethylamine N-oxide promotes antitumor immunity in triple-negative breast cancer, *Cell Metab.* 34 (4) (2022) 581–594, <https://doi.org/10.1016/j.cmet.2022.02.010>, e8.
- [9] D. Liu, AR pathway activity correlates with AR expression in a HER2-dependent manner and serves as a better prognostic factor in breast cancer, *Cell Oncol. (Dordr)* 43 (2) (2020) 321–333, <https://doi.org/10.1007/s13402-019-00492-6>.
- [10] L.S. Treviño, D.A. Gorelick, The interface of nuclear and membrane steroid signaling, *Endocrinology* 162 (8) (2021) bqab107, <https://doi.org/10.1210/endoqr/bqab107>.
- [11] A. Anestis, I. Zoi, A.G. Papavassiliou, M.V. Karamouzis, Androgen receptor in breast cancer-clinical and preclinical research insights, *Molecules* 25 (2) (2020) 358, <https://doi.org/10.3390/molecules25020358>.
- [12] C.P. You, M.H. Leung, W.C. Tsang, U.S. Khoo, H. Tsoi, Androgen Receptor as an Emerging Feasible Biomarker for Breast Cancer, *Biomolecules* 12 (1) (2022) 72, <https://doi.org/10.3390/biom12010072>.
- [13] G.K. Gupta, A.L. Collier, D. Lee, et al., Perspectives on triple-negative breast cancer: current treatment strategies, unmet needs, and potential targets for future therapies, *Cancers (Basel)* 12 (9) (2020) 2392, <https://doi.org/10.3390/cancers12092392>.
- [14] Y. Yuan, J.S. Lee, S.E. Yost, et al., A phase II clinical trial of pembrolizumab and enobosarm in patients with androgen receptor-positive metastatic triple-negative breast cancer, *Oncologist* 26 (2) (2021) 99–e217, <https://doi.org/10.1002/onco.13583>.
- [15] J.S. Prabhu, A. Korlimarla, S. Rajarajan, et al., Abstract PS6-55: the prognostic utility of AR/ER ratio in young women with breast cancer, *Cancer Res.* 81 (4 Suppl) (2021), <https://doi.org/10.1158/1538-7445.SABCS20-PS6-55>, PS6-55.
- [16] D. Basile, M. Cinausero, D. Iacono, et al., Androgen receptor in estrogen receptor positive breast cancer: beyond expression, *Cancer Treat Rev.* 61 (2017) 15–22, <https://doi.org/10.1016/j.ctrv.2017.09.006>.
- [17] M. Long, C. You, Q. Song, et al., AR expression correlates with distinctive clinicopathological and genomic features in breast cancer regardless of ESR1 expression status, *Int. J. Mol. Sci.* 23 (19) (2022) 11468, <https://doi.org/10.3390/ijms231911468>.
- [18] H. Yoshikawa, K. Nishino, H. Kosako, Identification and validation of new ERK substrates by phosphoproteomic technologies including Phos-tag SDS-PAGE, *J. Proteomics* 258 (2022) 104543, <https://doi.org/10.1016/j.jpro.2022.104543>.
- [19] S. Shi, T. Wu, Z. Ma, et al., Serum-derived extracellular vesicles promote the growth and metastasis of non-small cell lung cancer by delivering the m6A methylation regulator HNRNPC through the regulation of DLGP5, *J. Cancer Res. Clin. Oncol.* 149 (8) (2023) 4639–4651, <https://doi.org/10.1007/s00432-022-04375-6>.
- [20] X. Tang, H. Zhou, Y. Liu, High Expression of DLGP5 indicates poor prognosis and immunotherapy in lung adenocarcinoma and promotes proliferation through regulation of the cell cycle, *Dis. Markers* 2023 (2023) 9292536, <https://doi.org/10.1155/2023/9292536>.
- [21] X. Zeng, G. Shi, Q. He, P. Zhu, Screening and predicted value of potential biomarkers for breast cancer using bioinformatics analysis, *Sci. Rep.* 11 (1) (2021) 20799, <https://doi.org/10.1038/s41598-021-00268-9>.
- [22] Y. Weng, W. Liang, Y. Ji, et al., Key genes and prognostic analysis in HER2+ breast cancer, *Technol. Cancer Res. Treat.* 20 (2021) 1533033820983298, <https://doi.org/10.1177/1533033820983298>.
- [23] Y. Li, J. Wei, Y. Sun, et al., DLGP5 regulates the proliferation, migration, invasion, and cell cycle of breast cancer cells via the JAK2/STAT3 signaling axis, *Int. J. Mol. Sci.* 24 (21) (2023) 15819, <https://doi.org/10.3390/ijms242115819>.
- [24] J.M. Petrosino, J.Z. Longenecker, C.D. Angell, S.A. Hinger, C.R. Martens, F. Accornero, CGN2 participates in overload-induced skeletal muscle hypertrophy, *Matrix Biol.* 106 (2022) 1–11, <https://doi.org/10.1016/j.matbio.2022.01.003>.
- [25] S. Piya, T. Hawk, B. Patel, et al., Kinase-dead mutation: a novel strategy for improving soybean resistance to soybean cyst nematode *Heterodera glycines*, *Mol. Plant Pathol.* 23 (3) (2022) 417–430, <https://doi.org/10.1111/mpp.13168>.
- [26] K.U. Tufekci, B. Alural, E. Tarakcioglu, T. San, S. Genc, Lithium inhibits oxidative stress-induced neuronal senescence through miR-34a, *Mol. Biol. Rep.* 48 (5) (2021) 4171–4180, <https://doi.org/10.1007/s11033-021-06430-w>.
- [27] K. Cetkovašá, H. Šustová, S. Uldrijan, Ubiquitin-specific peptidase 48 regulates Mdm2 protein levels independent of its deubiquitinase activity, *Sci. Rep.* 7 (2017) 43180, <https://doi.org/10.1038/srep43180>.
- [28] J.J. Meijer, A. Leonetti, G. Airò, et al., Small cell lung cancer: novel treatments beyond immunotherapy, *Semin. Cancer Biol.* 86 (Pt 2) (2022) 376–385, <https://doi.org/10.1016/j.semcancer.2022.05.004>.
- [29] X. Wang, C. Wang, J. Guan, B. Chen, L. Xu, C. Chen, Progress of breast cancer basic research in China, *Int. J. Biol. Sci.* 17 (8) (2021) 2069–2079, <https://doi.org/10.7150/ijbs.60631>.
- [30] J. Blagih, M.D. Buck, K.H. Vousden, p53, cancer and the immune response, *J. Cell Sci.* 133 (5) (2020) jcs237453, <https://doi.org/10.1242/jcs.237453>.
- [31] J.S. Dolina, N. Van Braeckel-Budimir, G.D. Thomas, S. Salek-Ardakani, CD8<sup>+</sup> T cell exhaustion in cancer, *Front. Immunol.* 12 (2021) 715234, <https://doi.org/10.3389/fimmu.2021.715234>.
- [32] J. He, X. Xiong, H. Yang, et al., Defined tumor antigen-specific T cells potentiate personalized TCR-T cell therapy and prediction of immunotherapy response, *Cell Res.* 32 (6) (2022) 530–542, <https://doi.org/10.1038/s41422-022-00627-9>.
- [33] M.C. Sellars, C.J. Wu, E.F. Fritsch, Cancer vaccines: building a bridge over troubled waters, *Cell* 185 (15) (2022) 2770–2788, <https://doi.org/10.1016/j.cell.2022.06.035>.
- [34] F.J. Lowery, S. Krishna, R. Yossef, et al., Molecular signatures of antitumor neoantigen-reactive T cells from metastatic human cancers, *Science* 375 (6583) (2022) 877–884, <https://doi.org/10.1126/science.abc15447>.
- [35] D. Shetti, B. Zhang, C. Fan, C. Mo, B.H. Lee, K. Wei, Low dose of paclitaxel combined with XAV939 attenuates metastasis, angiogenesis and growth in breast cancer by suppressing Wnt signaling, *Cells* 8 (8) (2019) 892, <https://doi.org/10.3390/cells8080892>.

- [36] L. Hui, X. Shoumei, Z. Zhoujing, et al., Effects of androgen receptor overexpression on chondrogenic ability of rabbit articular chondrocytes, *Tissue Eng. Regen. Med.* 18 (4) (2021) 641–650, <https://doi.org/10.1007/s13770-021-00358-9>.
- [37] F. Peng, Q. Li, S.Q. Niu, et al., ZWINT is the next potential target for lung cancer therapy, *J. Cancer Res. Clin. Oncol.* 145 (3) (2019) 661–673, <https://doi.org/10.1007/s00432-018-2823-1>.
- [38] A. Ciupek, Y. Rechoum, G. Gu, et al., Androgen receptor promotes tamoxifen agonist activity by activation of EGFR in ER $\alpha$ -positive breast cancer, *Breast Cancer Res. Treat.* 154 (2) (2015) 225–237, <https://doi.org/10.1007/s10549-015-3609-7>.
- [39] R. Huang, J. Han, X. Liang, et al., Androgen receptor expression and bicalutamide antagonize androgen receptor inhibit  $\beta$ -catenin transcription complex in estrogen receptor-negative breast cancer, *Cell Physiol. Biochem.* 43 (6) (2017) 2212–2225, <https://doi.org/10.1159/000484300>.
- [40] X. Chen, M.M. Thiaville, L. Chen, et al., Defining NOTCH3 target genes in ovarian cancer, *Cancer Res.* 72 (9) (2012) 2294–2303, <https://doi.org/10.1158/0008-5472.CAN-11-2181>.
- [41] W. Xia, W. Chen, C. Ni, et al., Chemotherapy-induced exosomal circBACH1 promotes breast cancer resistance and stemness via miR-217/G3BP2 signaling pathway, *Breast Cancer Res.* 25 (1) (2023) 85, <https://doi.org/10.1186/s13058-023-01672-x>.
- [42] T. Xu, M. Dong, H. Li, R. Zhang, X. Li, Elevated mRNA expression levels of DLGAP5 are associated with poor prognosis in breast cancer, *Oncol. Lett.* 19 (6) (2020) 4053–4065, <https://doi.org/10.3892/ol.2020.11533>.
- [43] H. Zhang, Y. Liu, S. Tang, et al., Knockdown of DLGAP5 suppresses cell proliferation, induces G $_2$ /M phase arrest and apoptosis in ovarian cancer, *Exp. Ther. Med.* 22 (5) (2021) 1245, <https://doi.org/10.3892/etm.2021.10680>.
- [44] M.J. Ke, L.D. Ji, Y.X. Li, Bioinformatics analysis combined with experiments to explore potential prognostic factors for pancreatic cancer, *Cancer Cell Int.* 20 (2020) 382, <https://doi.org/10.1186/s12935-020-01474-7>.
- [45] Y. Sun, Q.M. Zhou, Y.Y. Lu, et al., Resveratrol inhibits the migration and metastasis of MDA-MB-231 human breast cancer by reversing TGF- $\beta$ 1-induced epithelial-mesenchymal transition, *Molecules* 24 (6) (2019) 1131, <https://doi.org/10.3390/molecules24061131>.
- [46] K.E. Craven, Y. Gökmen-Polar, S.S. Badve, CIBERSORT analysis of TCGA and METABRIC identifies subgroups with better outcomes in triple negative breast cancer, *Sci. Rep.* 11 (1) (2021) 4691, <https://doi.org/10.1038/s41598-021-83913-7>.
- [47] A. Butler, P. Hoffman, P. Smibert, E. Papalexli, R. Satija, Integrating single-cell transcriptomic data across different conditions, technologies, and species, *Nat. Biotechnol.* 36 (5) (2018) 411–420, <https://doi.org/10.1038/nbt.4096>.
- [48] P. Mistry, S. Nakabo, L. O'Neil, et al., Transcriptomic, epigenetic, and functional analyses implicate neutrophil diversity in the pathogenesis of systemic lupus erythematosus, *Proc. Natl. Acad. Sci. U.S.A.* 116 (50) (2019) 25222–25228, <https://doi.org/10.1073/pnas.1908576116>.
- [49] G. Yu, L.G. Wang, Y. Han, Q.Y. He, clusterProfiler: an R package for comparing biological themes among gene clusters, *OMICS* 16 (5) (2012) 284–287, <https://doi.org/10.1089/omi.2011.0118>.
- [50] A.M. Newman, C.B. Steen, C.L. Liu, et al., Determining cell type abundance and expression from bulk tissues with digital cytometry, *Nat. Biotechnol.* 37 (7) (2019) 773–782, <https://doi.org/10.1038/s41587-019-0114-2>.
- [51] D. Arunachalam, S.M. Ramanathan, A. Menon, et al., Expression of immune response genes in human corneal epithelial cells interacting with *Aspergillus flavus* conidia, *BMC Genomics* 23 (1) (2022) 5, <https://doi.org/10.1186/s12864-021-08218-5>.
- [52] T.R. Linkner, V. Ambrus, B. Kunkli, et al., Cellular Proteo-transcriptomic changes in the immediate early-phase of lentiviral transduction, *Microorganisms* 9 (11) (2021) 2207, <https://doi.org/10.3390/microorganisms9112207>.
- [53] Y.J. Deng, E.H. Ren, W.H. Yuan, G.Z. Zhang, Z.L. Wu, Q.Q. Xie, GRB10 and E2F3 as diagnostic markers of osteoarthritis and their correlation with immune infiltration, *Diagnostics (Basel)* 10 (3) (2020) 171, <https://doi.org/10.3390/diagnostics10030171>.
- [54] X.Y. Peng, Y. Wang, H. Hu, X.J. Zhang, Q. Li, Identification of the molecular subgroups in coronary artery disease by gene expression profiles, *J. Cell Physiol.* 234 (9) (2019) 16540–16548, <https://doi.org/10.1002/jcp.28324>.
- [55] C. Wang, N. Shen, Q. Guo, X. Tan, S. He, YAP/STAT3 inhibited CD8 $^+$  T cells activity in the breast cancer immune microenvironment by inducing M2 polarization of tumor-associated macrophages, *Cancer Med.* 12 (15) (2023) 16295–16309, <https://doi.org/10.1002/cam4.6242>.
- [56] B. Virassamy, F. Caramia, P. Savas, et al., Intratumoral CD8 $^+$  T cells with a tissue-resident memory phenotype mediate local immunity and immune checkpoint responses in breast cancer, *Cancer Cell* 41 (3) (2023) 585–601, <https://doi.org/10.1016/j.ccell.2023.01.004>, e8.
- [57] Y. Lee, H.K. Choi, K.P.U. N'deh, et al., Inhibitory effect of *Centella asiatica* extract on DNCB-induced atopic dermatitis in HaCaT cells and BALB/c mice, *Nutrients* 12 (2) (2020) 411, <https://doi.org/10.3390/nu12020411>.
- [58] Q. Fei, Y. Pan, W. Lin, et al., High-dimensional single-cell analysis delineates radiofrequency ablation induced immune microenvironmental remodeling in pancreatic cancer, *Cell Death Dis.* 11 (7) (2020) 589, <https://doi.org/10.1038/s41419-020-02787-1>.
- [59] M.E. Hoekstra, L. Bornes, F.E. Dijkgraaf, et al., Long-distance modulation of bystander tumor cells by CD8 $^+$  T cell-secreted IFN $\gamma$  [published correction appears in *Nat. Cancer.* 2020 Jul;1(7):749. 10.1038/s43018-020-0092-9], *Nat. Cancer* 1 (3) (2020) 291–301, <https://doi.org/10.1038/s43018-020-0036-4>.
- [60] K. Taniguchi, M. Karin, IL-6 and related cytokines as the critical lymphins between inflammation and cancer, *Semin. Immunol.* 26 (1) (2014) 54–74, <https://doi.org/10.1016/j.smim.2014.01.001>.
- [61] A. Brevi, L.L. Cogrossi, G. Grazia, et al., Much More Than IL-17A: cytokines of the IL-17 Family Between Microbiota and Cancer, *Front. Immunol.* 11 (2020) 565470, <https://doi.org/10.3389/fimmu.2020.565470>.
- [62] R. Campagna, V. Pozzi, S. Giorgini, et al., Paraoxonase-2 is upregulated in triple negative breast cancer and contributes to tumor progression and chemoresistance, *Hum. Cell* 36 (3) (2023) 1108–1119, <https://doi.org/10.1007/s13577-023-00892-9>.
- [63] F. Li, Y. Zhang, Y. Shi, S. Liu, Comprehensive analysis of prognostic and immune infiltrates for RAD51 in human breast cancer, *Crit. Rev. Eukaryot. Gene. Expr.* 31 (4) (2021) 71–79, <https://doi.org/10.1615/CritRevEukaryotGeneExpr.2021038876>.
- [64] E. Vagia, D. Mahalingam, M. Cristofanilli, The landscape of targeted therapies in TNBC, *Cancers (Basel)* 12 (4) (2020) 916, <https://doi.org/10.3390/cancers12040916>.
- [65] A. Reiter, J. Gotlib, I. Álvarez-Twose, et al., Efficacy of avapritinib versus best available therapy in the treatment of advanced systemic mastocytosis, *Leukemia* 36 (8) (2022) 2108–2120, <https://doi.org/10.1038/s41375-022-01615-z>.
- [66] H. Yako-Suketomo, K. Katayama, A. Ogihara, M. Asai-Sato, Process of developing a cervical cancer education program for female university students in a health and physical education teacher training course: an action research, *BMC Womens Health* 23 (1) (2023) 169, <https://doi.org/10.1186/s12905-023-02273-8>.
- [67] M. Sánchez-Ortega, A.C. Carrera, A. Garrido, Role of NRF2 in lung cancer, *Cells* 10 (8) (2021) 1879, <https://doi.org/10.3390/cells10081879>.
- [68] D.C. Yu, X.Y. Chen, H.Y. Zhou, et al., TRIP13 knockdown inhibits the proliferation, migration, invasion, and promotes apoptosis by suppressing PI3K/AKT signaling pathway in U2OS cells, *Mol. Biol. Rep.* 49 (4) (2022) 3055–3064, <https://doi.org/10.1007/s11033-022-07133-6>.
- [69] Y.T. Chiang, Y.C. Chien, Y.H. Lin, H.H. Wu, D.F. Lee, Y.L. Yu, The function of the mutant p53-R175H in cancer, *Cancers (Basel)* 13 (16) (2021) 4088, <https://doi.org/10.3390/cancers13164088>.
- [70] P. Lotfinejad, T. Kazemi, A. Mokhtarzadeh, et al., PD-1/PD-L1 axis importance and tumor microenvironment immune cells, *Life Sci.* 259 (2020) 118297, <https://doi.org/10.1016/j.lfs.2020.118297>.